Title
Evaluating the Stability of Single-Atom Catalysts with High Chemical Activity

Journal
The Journal of Physical Chemistry C, 122(38)

ISSN
1932-7447

Authors
Wang, Chen Santillan
Wang, Hui
Wu, Ruqian
et al.

Publication Date
2018-09-27

DOI
10.1021/acs.jpcc.8b06621

Peer reviewed

THE JOURNAL OF PHYSICAL CHEMISTRY C

Article

Cite This: J. Phys. Chem. C 2018, 122, 21919−21926

pubs.acs.org/JPCC

Evaluating the Stability of Single-Atom Catalysts with High Chemical Activity

Chen Santillan Wang,[†] Hui Wang,[‡] Ruqian Wu,[‡] and Regina Ragan*[,†]

[†]Department of Chemical Engineering and Materials Science, University of California, Irvine, Irvine, California 92697-2575, United States

[‡]Department of Physics and Astronomy, University of California, Irvine, Irvine, California 92697-4575, United States

ABSTRACT: Single-atom catalysts represent the most efficient use of precious metals while at the same time offering the potential for high catalytic activity. Yet it has proven challenging to identify supports enabling high catalytic activity while at the same time inhibiting aggregation of metal adatoms. Density functional theory calculations are employed to identify how the local molecular environment on graphene can be used to stabilize a single platinum adatom and provide favorable activity for a benchmark reaction, CO oxidation. Graphene is modified via defects and dopants—specifically single vacancy and pyridinic N-doping—so that we can see how the electronic structure and chemical activity of Pt atoms are affected. The ability to disperse single atoms on graphene supports is examined by comparing binding energy of Pt atoms at neighboring stable sites versus isolated sites and evaluating the tendency toward clustering. Nudged elastic band calculations indicate that pyridinic N-doped graphene is a promising candidate to support a single Pt atom acting as a catalyst that is resistant to poisoning and enhances CO oxidation efficiency.

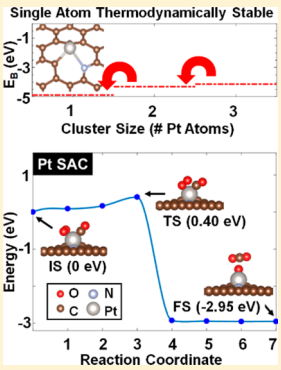

INTRODUCTION

Supported noble-metal catalysts—such as platinum, gold, and palladium—are widely used in industry due to their high activity and selectivity for a broad range of chemical reactions. Applications include chemical transformation, energy conversion, and environmental remediation.[1−7] As known, the active sites on a catalyst are primarily composed of the surface-most atoms: atoms that are inaccessible in the bulk largely provide only mechanical support. Inspired by visions of minimizing the number of noble metal (e.g., Pt) atoms so the surface to volume ratio can reach its ultimate limit, extensive studies have been performed to explore the possibility of developing single-atom catalysts.[8−14] One of the main practical challenges in this realm is how to disperse single atoms that are resistant to aggregation on support surfaces using standard deposition methods.[15−18] Graphene is a promising substrate due to its naturally high structural stability. However, experiments have shown that Pt and other metals tend to aggregate and form clusters on pristine graphene surfaces due to the shallow energy barriers for the segregation of metal adatoms.[19,20] The strong interaction between vacancies and dopants with metallic adatoms on graphene appears to be essential for anchoring single Pt adatoms.[21−25] At the same time, the molecular environment on modified graphene may enhance electronic and chemical activity of Pt adatoms. For example, prior experimental results indicate that pyridinic N-doped graphene is more catalytically active than graphene with a single vacancy defect.[26,27] While several first-principles calculations of gold, copper, and iron on graphene predicted high activity of these systems for the CO oxidation reaction,[28−30] the tendency for metal atom aggregations has rarely been discussed. This inspires us to investigate the stability of small Pt clusters and their catalytic activities on different molecular environments.

In the present work, we first explore the tendency for Pt adatoms to form clusters on graphene by using density functional theory (DFT) calculations. From the relative binding energies, we estimate the potential for aggregation of Pt atoms on pristine, single vacancy, and pyridinic N-doped graphene (denoted as PG, SVG, and PNG, respectfully). This goes beyond the previous theoretical efforts that mainly optimize stable cluster sizes and geometries in vacuum.[31−33] Specially, we found that Pt prefers to individually take defect sites on graphene so the single-atom catalyst (SAC) can be synthesized when the Pt coverage is smaller than the defect density. To demonstrate the catalytic activity of SAC, we simulate the oxidation of CO which is often used as a benchmark catalytic reaction due to its simplicity and technological importance.[34−39] Indeed, results suggest that Pt_1/PNG stretches the O_2 bond length, thereby lowering the activation barrier for the molecule's dissociation and enhancing CO oxidation efficiency. Our study thus adds a new choice for the design of effective catalysts for the reduction of environmental pollution caused by CO emission from vehicular, industrial, and other processes.[40−44]

Received: July 11, 2018
Revised: August 25, 2018
Published: August 31, 2018

DOI: 10.1021/acs.jpcc.8b06621
J. Phys. Chem. C 2018, 122, 21919−21926

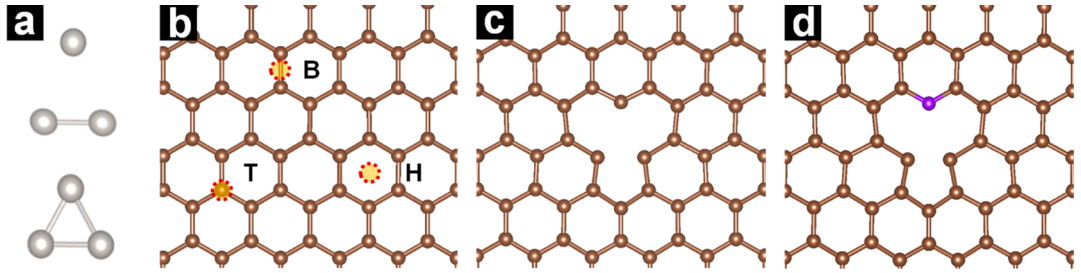

Figure 1. Optimized DFT models of: (a) platinum clusters of 1, 2, and 3 atoms in size relaxed in vacuum; (b) pristine graphene; (c) single vacancy graphene; and (d) pyridinic N-doped graphene. Top (T), bridge (B), and hollow (H) sites are highlighted in (b).

COMPUTATIONAL METHODS

Density functional theory calculations were performed by the Vienna *ab initio* Simulation Package (VASP) for all calculations presented here.[45,46] Projector-augmented wave (PAW) potentials describe the ion cores;[47,48] exchange and correlation terms are described via the Perdew–Burke–Ernzerhof functional.[49] All simulations apply a 6 × 6 graphene supercell with a vacuum layer of 15 Å to avoid spurious interaction. The energy cutoff for the plane-wave expansion in all the calculations is 500 eV. Brillouin zone sampling is done using the Monkhorst–Pack[50] with a 5 × 5 × 1 grid for relaxation and a 9 × 9 × 1 grid for density of states calculations. Structures were relaxed until the force on each atom was smaller than 0.02 eV/Å. Binding energy E_B is defined with the expression

$$E_B = (E_{m\text{-}g} - E_g - E_m)/n \quad (1)$$

where $E_{m\text{-}g}$, E_g, and E_m represent the total energies of the adsorbate on the modified-graphene full system, the free-standing modified graphene, and the metal adatom, respectively. Charge transfer between the adatom and graphene is visualized via charge density difference plots using VESTA 3 software[51] according to the following expression

$$\Delta n(r) = n_{m\text{-}g}(r) - n_g(r) - n_m(r) \quad (2)$$

where $n_{m\text{-}g}$, n_g, and n_m represent charge densities of the adsorbate on the modified-graphene full system, the free-standing modified graphene, and the metal adatom, respectively.

Finally, nudged elastic band (NEB) calculations[52] were performed using VASP Transition State Theory (VTST) tools developed by Jónsson et al.[52,53] and maintained by Henkelman et al.[45,54−56]

RESULTS AND DISCUSSION

First, stable atomic arrangements and electronic structures of small ensembles of Pt atoms are investigated on pristine graphene surfaces and then modified with vacancy defects and dopants. Specifically, the systems investigated are (shown in Figure 1) (a) Pt_n clusters (n = 1, 2, 3) with structures relaxed in vacuum, for reference, and the substrate supports that include (b) pristine graphene (PG), (c) single vacancy graphene (SVG), and (d) pyridinic nitrogen-doped graphene (PNG). In the last case, a carbon double vacancy in the graphene lattice reconstructs in the presence of a nitrogen dopant, breaking the 6-fold lattice symmetry and forming a "pyridinic nitrogen" configuration of 6 and 5 element rings. PNG is commonly observed in scanning tunneling microscopy (STM) investigations of nitrogen-doped graphene systems.[57−59] When examining variations in catalytic activity as a function of Pt cluster size and electronic structure of graphene supports, it is critical to also evaluate the stability of clusters from trimers down to a single Pt atom on graphene. Examining the preference of stabilizing an isolated atom versus cluster formation during a deposition process is critical in evaluating feasibility.

Establishing Binding Sites on Graphene Surfaces. One of the major roadblocks in implementing single-atom catalysis is that even if single atoms are deposited on a substrate these isolated atoms often prefer to migrate and eventually aggregate into clusters on the surface.[19,20] Here the potential of migration and cluster formation is examined by considering interactions between nearby Pt atoms, each at neighboring stable sites. In the case of a single adatom on PG, there are three possible adsorption sites: top (directly sitting above a carbon atom), bridge (located above a carbon–carbon bond), and hollow (which is at the center of a hexagon in the carbon honeycomb lattice). These sites are highlighted in Figure 1b and labeled T, B, and H, respectively. Binding energies (E_B) and the distances between the Pt_n cluster and neighboring C atoms (d_{Pt-C}) are calculated to characterize the stability of Pt at sites of interest in the graphene substrates. The most stable position for a Pt adatom is at the bridge site, having an E_B of −1.53 eV and a d_{Pt-C} of 2.1 Å, which is in accordance with previous reports.[31,60−62] The top site is nearly just as favorable. Nudged elastic band calculations determined that the energy barrier for Pt to migrate between two neighboring bridge sites by passing through a metastable top site on PG is 0.16 eV, as shown in Figure 2a. This value is similar to the BE difference calculated by Fampiou et al.[33] At room temperature, this energy value difference corresponds roughly to a Pt atom hopping 20 times every second,[16] which means that Pt migration will occur and Pt clustering is inevitable.

The next step is to compare how the E_B of Pt atoms varies with cluster size. The evaluation for forming a dimer begins with the optimized single-atom configuration and considers energy barriers for Pt migration to all symmetrically equivalent neighboring stable sites (top and bridge) in the honeycomb lattice as well as the site directly atop the original Pt atom as viable locations to add a second Pt atom. Figure 2b depicts Pt atom migration along the stable bridge and metastable top sites. For trimers, this process is repeated beginning with the optimized dimer configuration.

When considering two Pt atoms, the E_B and distance to the substrate both increase to −2.19 eV and 2.22 Å, respectively, suggesting that the increase in E_B results from Pt–Pt interaction rather than Pt–C interaction. The addition of a third Pt atom further increases the E_B of the overall cluster to −2.88 eV/atom, while the Pt–C distance remains the same

DOI: 10.1021/acs.jpcc.8b06621
J. Phys. Chem. C 2018, 122, 21919−21926

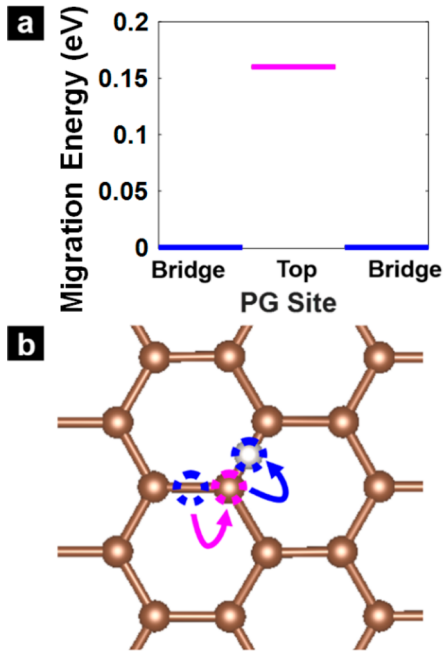

Figure 2. Schematic depicting energetically favorable Pt migration path on PG to evaluate tendency for clustering. Arrows depict migration path of Pt through bridge and top sites (denoted by blue and pink dotted circles, respectively).

(2.22 Å). These findings are summarized in Figure 3 and in accordance with the literature.[60−62] Unsurprisingly results indicate that Pt prefers to cluster on PG and is stabilized by

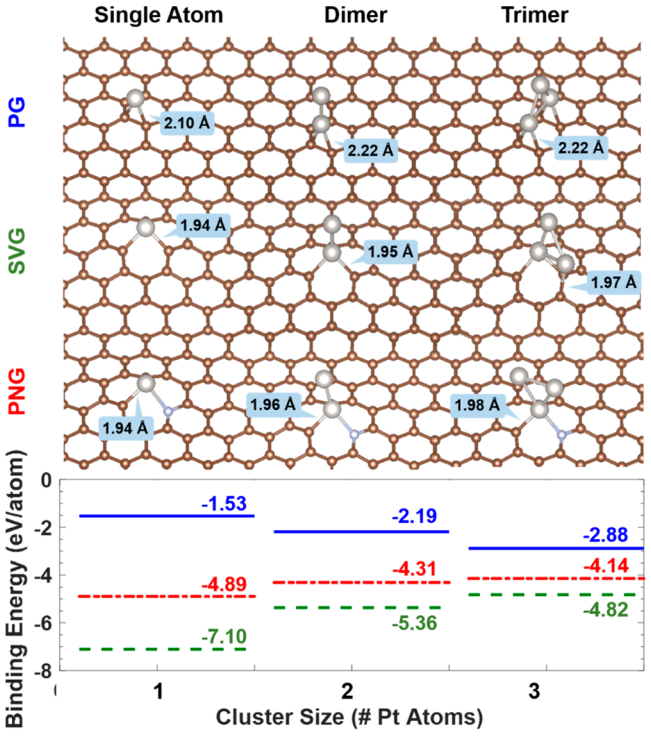

Figure 3. Schematic depicting the most energetically stable cluster geometries for Pt clusters of 1−3 atoms on PG, SVG, and PNG substrates. Text bubbles in light blue indicate the d_{Pt-C} for each system. Binding energies as a function of cluster size are plotted below with PG in solid blue, SVG in dashed green, and PNG in dotted red.

interactions with other Pt atoms, rather than solely interacting with the graphene substrate as an isolated adatom. These results show PG is unsuitable for anchoring isolated Pt and facilitating single-atom catalysis. More importantly, the agreement of these results with experimentally observed clusters establishes that our methodology is useful in evaluating other substrates.

Single Vacancy Graphene. Conversely, when this methodology is applied on SVG it affirms its potential as a support structure for stabilizing Pt SACs. This is significant as SVG substrates have been observed to support catalytically active metal nanoclusters.[32,33] The trapping ability of that vacant site present in the SVG and PNG systems is reflected by large E_B values, −7.10 eV and −4.89, respectively, also shown in Figure 3. Charge density difference plots are generated by subtracting the superposition of the respective charge densities of the individual adsorbate and the substrate and provide insight into the resultant high E_B by observing the spatial redistribution of charge density as an adsorbate binds to a substrate surface. As shown in Figure 4, the presence of

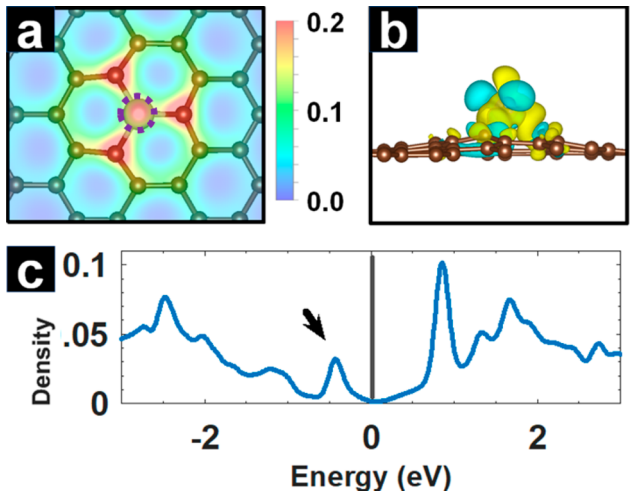

Figure 4. Charge maps (a), charge density difference plots (b), and DOS plots (c) for a Pt atom, indicated with the dashed purple circle in (a) adsorbed on SVG. The charge maps are plotted in units of e/Bohr^3. In the charge density difference plots, yellow and blue represent charge accumulation and depletion, respectively. The DOS plots reflect the number of states/eV for the total DOS of the system, where the Fermi level is set to 0 eV.

vacancy defects in the graphene honeycomb lattice provides dangling bonds which induce charge on adjacent C atoms and influence these electron-deficient atoms to stabilize themselves by bonding with Pt. For a single Pt atom on SVG, the adsorbate binds to the vacant site, shifting out of plane from the honeycomb lattice by a height of 1.03 Å due the atom's size mismatch.[63−65] Upon increasing the cluster size to two or three atoms, a single Pt atom anchors the rest of the cluster at the defect site, and d_{Pt-C} hardly changes. For the dimer and trimer Pt, the E_B decreases to −5.36 and −4.82 eV, respectively. These values, also shown in Figure 3, indicate that Pt atoms energetically prefer to find separate vacancy sites rather than cluster together at one vacancy site. It is important to note that the ability to isolate Pt atoms on SVG is coverage dependent.[66] Clearly, the Pt surface coverage and vacancy density must be comparable if one wants to produce Pt_1/SVG configurations for catalysis. For PNG, which will be discussed

DOI: 10.1021/acs.jpcc.8b06621
J. Phys. Chem. C 2018, 122, 21919−21926

below, the N to C ratio is 1.4%. This value corresponds roughly to a typical dopant density in N-doped graphene.[67,68] Thus, the desired atomic ratio of Pt to C is ≤1.4%, and results will show that these incredibly low concentrations of Pt enable favorable catalytic activity.

While Pt is a well-known catalyst often used in industrial applications, previous research has shown that only atomic sites with specific coordination participate in enhancing reactions.[69−71] Thus, it is important to examine the electronic structures of the Pt_1/SVG system via density of states (DOS) plots in order to understand its ability for promoting chemical reactions and use it as a benchmark for understanding less explored systems. The broadened Pt states overlap with the total DOS lying around the Fermi energy, an indication of strong hybridization between the Pt and the neighboring C atom that has been previously observed in theoretical studies.[72] As observed in Figure 4, there is a pronounced peak at 0.46 eV below the Fermi energy (indicated in Figure 4c with an arrow), which other studies have shown allows for weak CO adsorption and facilitates the O_2 adsorption, enhancing the catalytic activity for CO oxidation and methanol oxidation.[73,74]

Pyridinic N-Doped Graphene. There are numerous theoretical studies exploring properties of Pt on PG, SVG, and N-doped graphene surfaces where a N atom hetero-substitutes a C atom. Surprisingly, adatom properties on N-doped pyridinic configuration have been less explored[75,76] though PNG is a structure commonly observed in STM investigations of nitrogen-doped graphene systems.[57−59] Interestingly, X-ray photoelectron spectroscopy studies have identified PNG as highly catalytically active on its own.[26,27] It has been reported that the presence of pyridinic-N influences the local electronic structure, increasing the density of π states near the Fermi level and lowering the work function.[77] For these reasons, PNG is a promising substrate to consider for single Pt atom catalysis. The results of E_B as a function of cluster size using the analysis discussed above show that it is also a suitable candidate for stabilizing a single Pt atom. As shown in Figure 3, the addition of Pt atoms decreases E_B and increases d_{Pt-C}, indicating the Pt atoms prefer to distribute themselves among separate PNG sites.

On PNG, nitrogen contributes more electrons than is reciprocated by the adjacent carbons, which use an sp^3-hybridized orbital to bond with the N atom due to the resulting underutilization of its 2pz orbital.[78] In the case of Pt_1/PNG, the N and Pt insert themselves into the two carbon vacancies, sinking in plane and reforming the honeycomb lattice. As seen in Figure 5a and b, excess charge from N weakly interacts with the Pt; instead Pt strongly attracts to the dangling bonds of the neighboring carbons, resulting in an E_B of −4.89 eV. Although this value is lower than that for the SVG case, the d_{Pt-C} bond length is the same for both supports, indicating the favorability of reconstructing the honeycomb lattice.

The addition of a dopant N atom strongly influences the electronic structure, which deviates greatly from that for SVG. Interestingly, Pt_1/PNG is magnetic largely due to the contribution of the N and Pt atoms, with a spin magnetic moment of 0.82 μ_B. There are two peaks, at 0.15 eV below the Fermi level in the spin down channel and on the up spin 0.31 eV above the Fermi level in the spin up channel (Figure 5c), which should have important consequences for enhancing catalytic activity.

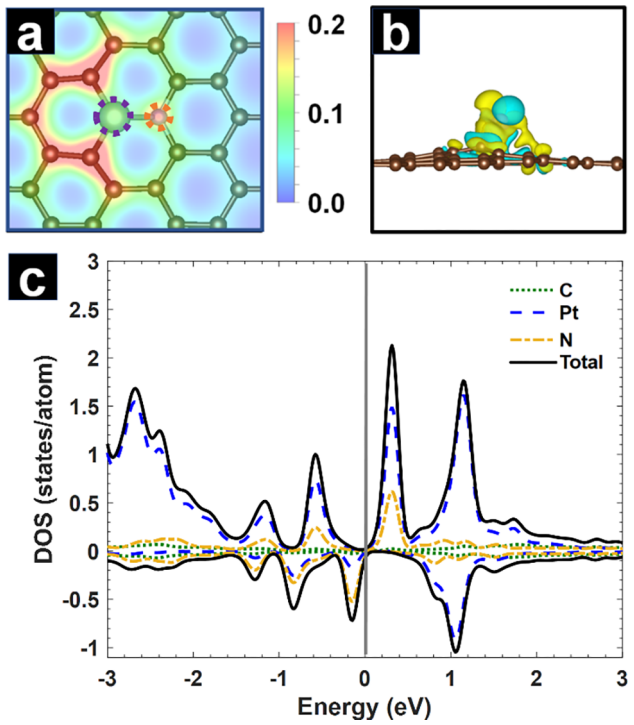

Figure 5. Charge maps (a), charge density difference plots (b), and density of states plots (c) for a Pt atom (indicated with a dashed purple circle) adsorbed on pyridinic N-doped graphene (where the N atom is indicated with a dashed orange circle). The charge maps are plotted in units of e/Bohr^3. In the charge density difference plots, yellow and blue represent charge accumulation and depletion, respectively.

Investigations of Chemical Activity and CO Oxidation. The chemical activity of these configurations was investigated, first by observing the binding energetics with small molecules and then as a catalyst for CO oxidation. The adsorption geometry and the energetics of the following gas molecules were investigated for H_2, O_2, H_2O, CO, and CO_2 on Pt_1/PNG. The study of these molecules facilitates the investigation of hydrogen evolution (HER) and carbon monoxide oxidation reactions; while relatively simple systems, they are chosen for their widespread importance.[1,79] Efficient catalysis of HER is a major necessary step in developing clean, renewable fuel resources, and catalysis of CO oxidation is incredibly important in reducing the toxicity of exhaust emissions from automobiles.[39]

Minimizing the total energy, the most stable adsorption geometry of each gas molecule on the single Pt adatom was determined. The binding energies of each of these molecules are summarized in Table 1, according to the following equation

$$E_{ads} = E_{g/Pt/PNG} - E_g - E_{Pt/PNG} \quad (3)$$

Table 1. Binding Energies of Molecules to Pt_1/PNG

	binding energy (eV)
H_2	−1.484
O_2	−1.533
H_2O	−0.345
CO	−1.819
CO_2	−0.559

DOI: 10.1021/acs.jpcc.8b06621
J. Phys. Chem. C 2018, 122, 21919−21926

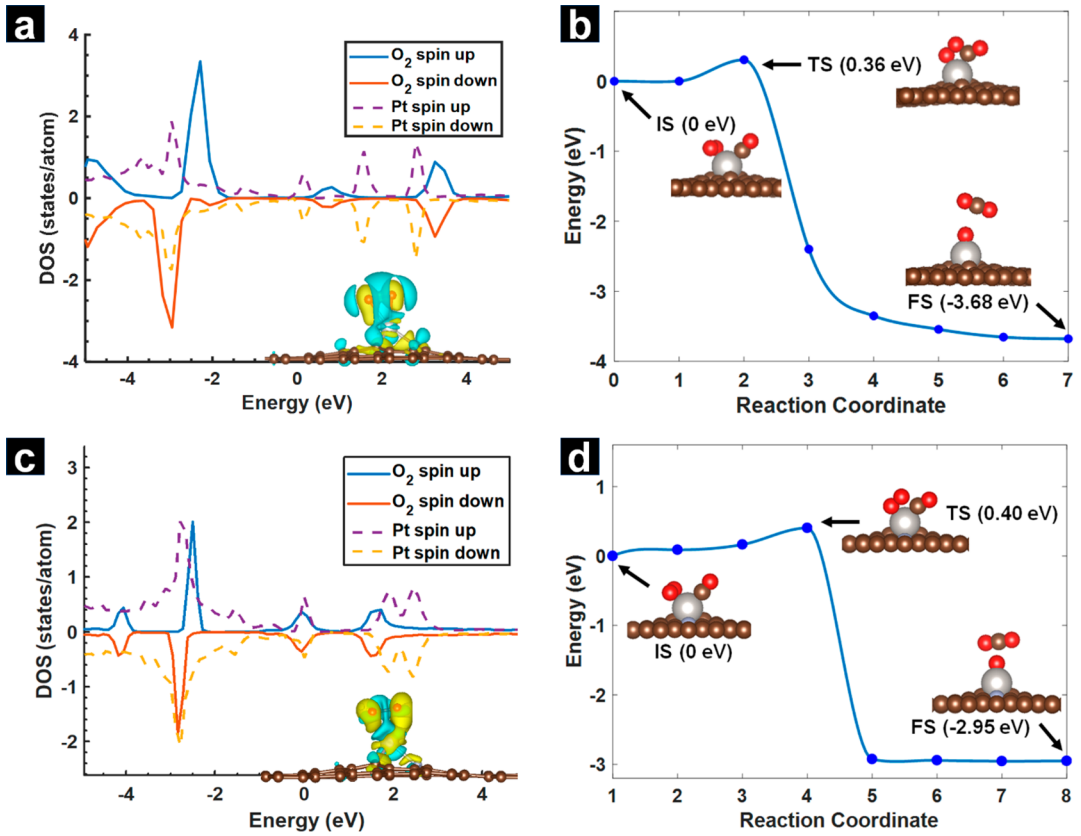

Figure 6. (a) Density of states projected for different atoms are found with the Fermi level (placed at 0 eV) for Pt_1/SVG. (b) Optimized structures of CO oxidation on the Pt_1/SVG demonstrate the Langmuir−Hinshelwood reaction including the initial state (IS), transition state (TS), and final state (FS). Red, brown, and gray balls represent oxygen, carbon and Pt atoms, respectively. (c) The density of states projected for different atoms is found with the Fermi level (placed at 0 eV) for Pt_1/PNG. (d) Optimized structures of CO oxidation on the Pt_1/PNG demonstrate the Langmuir−Hinshelwood reaction including the initial state (IS), transition state (TS), and final state (FS). Red, brown, and gray balls represent oxygen, carbon and Pt atoms, respectively.

where $E_{g/Pt/PNG}$, E_g, and $E_{Pt/PNG}$ represent the total energies of the gas molecules adsorbed on Pt_1/PNG, the free gas molecule in vacuum, and the Pt_1/PNG system, respectively.

Through studies of various adsorption sites, the most stable configuration for each adsorbate is obtained. Table 1 reveals a high value of E_{ads} for H_2, which results from the Pt interacting with each H atom such that the molecule's bond length is stretched. This explains the observed catalytic activity of Pt_1/PNG for the hydrogen evolution reaction in which H_2 dissociates through charge donation via the Pt atom.[80] Similarly, Table 1 reveals that the E_{ads} for CO and O_2 is relatively high compared to that for CO_2, and this finding suggests the possible enhancement for CO to CO_2 conversion or CO to fuel conversion through a few hydrogenation steps. The C−O bond length maintains almost the same as that of an isolated CO molecule after adsorption; in contrast, as shown in Figure 6a, O_2 adsorbs to the Pt atom and parallel to the plane of the graphene, increasing its bond length from 1.24 to 1.44 Å due to the electronic charge transfer from the Pt atom to the $2\pi^*$ orbital of O_2.

These energy and length values are similar to that for Pt_1/SVG, a system which has been predicted to catalyze CO oxidation via the Langmuir−Hinshelwood mechanism.[74] As shown in Figure 6b, calculations here predict a 0.36 eV energy barrier for this reaction. It would therefore be interesting to see if Pt_1/PNG can also facilitate this reaction. The rate-limiting step in the reaction is the dissociation of the oxygen molecule, which is found here to have a prohibitively high dissociation energy of 6.66 eV when calculated for an O_2 molecule in the gas phase.[81] However, in weakening the O_2 bond, this dissociation energy is significantly decreased in the presence of the Pt_1/PNG catalyst. The CO oxidation reaction pathway can be traced using the NEB method, as shown in Figure 6d. Both CO and O_2 are stable when coadsorbed on Pt_1/PNG, forming the initial state (IS) of the reaction. In this configuration, the bond length of the O_2 molecule remains stretched, while the E_{ads} value decreases to 0.61 eV. Throughout the reaction, one of the oxygen atoms begins approaching the carbon atom of CO, eventually forming the transition state (TS) with an energy barrier of 0.40 eV, where the O−O bond is elongated to 1.67 Å and a peroxo-type O−O−C−O complex is formed over the Pt atom. Afterward, the O−O bond dissociates entirely, allowing the CO_2 molecule to form, which drops the energy of the system by 3.93 eV. The 0.40 eV energy barrier for the reaction is a modest one and comparable to the 0.36 eV energy barrier determined for the Pt_1/SVG system. The remaining O adsorbate can easily be reacted with another CO molecule via the Eley−Rideal mechanism, thus allowing the catalyst to be reusable.[74]

CONCLUSION

In summary, DFT calculations have been applied to investigate the feasibility of stabilizing a Pt SAC on pristine, defected, and doped graphene supports. The different graphene substrates

DOI: 10.1021/acs.jpcc.8b06621
J. Phys. Chem. C 2018, 122, 21919−21926

influence the local electronic structure of Pt atoms on the surface and result in varying catalytic activities. By examining an energetically favorable migration path on the supports, this work has identified that PNG supports are favorable to both isolate a single Pt atom and to tune the electronic structure for high catalytic efficiency. The Pt−C interaction of the adsorbed Pt atom at the vacant site of the honeycomb lattice is responsible for the strong binding and stabilization of a single Pt atom on the SVG and PNG substrates and for facilitating charge transfer between Pt and O_2, which increases the efficiency of the rate-limiting step in the oxidation reaction. NEB calculations show that Pt_1/SVG and Pt_1/PNG exhibit high catalytic activity for CO oxidation with a modest energy barrier of 0.36 and 0.40 eV, respectively. At the same time, the remaining O adsorbate is available to react with another CO molecule via the Eley−Rideal mechanism, indicating that the SAC is resistant to poisoning. Compared to other support systems such as carbon sheets, both Pt_1/SVG and Pt_1/PNG systems offer prime candidates for SAC. Overall these results present an important perspective when designing SAC on supports: not only is catalytic activity important but also stability of an isolated adatom.

AUTHOR INFORMATION

Corresponding Author

*E-mail: rragan@uci.edu.

ORCID

Hui Wang: 0000-0001-9972-2019

Regina Ragan: 0000-0002-8694-5683

Notes

The authors declare no competing financial interest.

ACKNOWLEDGMENTS

We thank Z. Lu and J. Li for insightful comments. This material is based upon work supported by the National Science Foundation Graduate Research Fellowship under Grant No. DGE-1321846 and the fund for Chemical Innovation on Chemistry at the Space-Time Limit (CaSTL) under Grant No. CHE-1414466. This work used the Extreme Science and Engineering Discovery Environment (XSEDE), which is supported by National Science Foundation Grant No. ACI-1548562. The allocation accounts used in this research were CHE140084 and DMR150047.

REFERENCES

(1) Bell, A. T. The Impact of Nanoscience on Heterogeneous Catalysis. *Science* **2003**, *299* (5613), 1688−1691.

(2) Zhang, J.; Sasaki, K.; Sutter, E.; Adzic, R. R. Stabilization of Platinum Oxygen-Reduction Electrocatalysts Using Gold Clusters. *Science* **2007**, *315* (5809), 220−222.

(3) Vajda, S.; Pellin, M. J.; Greeley, J. P.; Marshall, C. L.; Curtiss, L. A.; Ballentine, G. A.; Elam, J. W.; Catillon-Mucherie, S.; Redfern, P. C.; Mehmood, F.; et al. Subnanometre Platinum Clusters as Highly Active and Selective Catalysts for the Oxidative Dehydrogenation of Propane. *Nat. Mater.* **2009**, *8* (3), 213−216.

(4) Zang, W.; Li, G.; Wang, L.; Zhang, X. Catalytic Hydrogenation by Noble-Metal Nanocrystals with Well-Defined Facets: A Review. *Catal. Sci. Technol.* **2015**, *5* (5), 2532−2553.

(5) Fan, Z.; Zhang, H. Template Synthesis of Noble Metal Nanocrystals with Unusual Crystal Structures and Their Catalytic Applications. *Acc. Chem. Res.* **2016**, *49* (12), 2841−2850.

(6) Hutchings, G.; Catlow, R.; Hardacre, C.; Collier, P. *Modern Developments In Catalysis*; World Scientific, 2016.

(7) Wang, Y.; Arandiyan, H.; Scott, J.; Bagheri, A.; Dai, H.; Amal, R. Recent Advances in Ordered Meso/Macroporous Metal Oxides for Heterogeneous Catalysis: A Review. *J. Mater. Chem. A* **2017**, *5* (19), 8825−8846.

(8) Liu, S.; Huang, S. Theoretical Insights into the Activation of O2 by Pt Single Atom and Pt4 Nanocluster on Functionalized Graphene Support: Critical Role of Pt Positive Polarized Charges. *Carbon* **2017**, *115*, 11−17.

(9) Cui, X.; Junge, K.; Dai, X.; Kreyenschulte, C.; Pohl, M.-M.; Wohlrab, S.; Shi, F.; Brückner, A.; Beller, M. Synthesis of Single Atom Based Heterogeneous Platinum Catalysts: High Selectivity and Activity for Hydrosilylation Reactions. *ACS Cent. Sci.* **2017**, *3* (6), 580−585.

(10) DeRita, L.; Dai, S.; Lopez-Zepeda, K.; Pham, N.; Graham, G. W.; Pan, X.; Christopher, P. Catalyst Architecture for Stable Single Atom Dispersion Enables Site-Specific Spectroscopic and Reactivity Measurements of CO Adsorbed to Pt Atoms, Oxidized Pt Clusters, and Metallic Pt Clusters on TiO2. *J. Am. Chem. Soc.* **2017**, *139* (40), 14150−14165.

(11) Qiao, B.; Wang, A.; Yang, X.; Allard, L. F.; Jiang, Z.; Cui, Y.; Liu, J.; Li, J.; Zhang, T. Single-Atom Catalysis of CO Oxidation Using Pt1/FeOx. *Nat. Chem.* **2011**, *3* (8), 634−641.

(12) Sun, S.; Zhang, G.; Gauquelin, N.; Chen, N.; Zhou, J.; Yang, S.; Chen, W.; Meng, X.; Geng, D.; Banis, M. N.; et al. Single-Atom Catalysis Using Pt/Graphene Achieved through Atomic Layer Deposition. *Sci. Rep.* **2013**, DOI: 10.1038/srep01775.

(13) Yang, X.-F.; Wang, A.; Qiao, B.; Li, J.; Liu, J.; Zhang, T. Single-Atom Catalysts: A New Frontier in Heterogeneous Catalysis. *Acc. Chem. Res.* **2013**, *46* (8), 1740−1748.

(14) Thomas, J. M.; Saghi, Z.; Gai, P. L. Can a Single Atom Serve as the Active Site in Some Heterogeneous Catalysts? *Top. Catal.* **2011**, *54* (10−12), 588−594.

(15) López-Cudero, A.; Solla-Gullón, J.; Herrero, E.; Aldaz, A.; Feliu, J. M. CO Electrooxidation on Carbon Supported Platinum Nanoparticles: Effect of Aggregation. *J. Electroanal. Chem.* **2010**, *644* (2), 117−126.

(16) Muhich, C. L.; Westcott, J. Y.; Morris, T. C.; Weimer, A. W.; Musgrave, C. B. The Effect of N and B Doping on Graphene and the Adsorption and Migration Behavior of Pt Atoms. *J. Phys. Chem. C* **2013**, *117* (20), 10523−10535.

(17) Hansen, T. W.; DeLaRiva, A. T.; Challa, S. R.; Datye, A. K. Sintering of Catalytic Nanoparticles: Particle Migration or Ostwald Ripening? *Acc. Chem. Res.* **2013**, *46* (8), 1720−1730.

(18) Johns, T. R.; Goeke, R. S.; Ashbacher, V.; Thüne, P. C.; Niemantsverdriet, J. W.; Kiefer, B.; Kim, C. H.; Balogh, M. P.; Datye, A. K. Relating Adatom Emission to Improved Durability of Pt−Pd Diesel Oxidation Catalysts. *J. Catal.* **2015**, *328*, 151−164.

(19) Uzun, A.; Ortalan, V.; Browning, N. D.; Gates, B. C. A Site-Isolated Mononuclear Iridium Complex Catalyst Supported on MgO: Characterization by Spectroscopy and Aberration-Corrected Scanning Transmission Electron Microscopy. *J. Catal.* **2010**, *269* (2), 318−328.

(20) Uzun, A.; Ortalan, V.; Hao, Y.; Browning, N. D.; Gates, B. C. Nanoclusters of Gold on a High-Area Support: Almost Uniform Nanoclusters Imaged by Scanning Transmission Electron Microscopy. *ACS Nano* **2009**, *3* (11), 3691−3695.

(21) Kim, G.; Jhi, S.-H. Carbon Monoxide-Tolerant Platinum Nanoparticle Catalysts on Defect-Engineered Graphene. *ACS Nano* **2011**, *5* (2), 805−810.

(22) Zhou, M.; Zhang, A. H.; Dai, Z. X.; Zhang, C.; Feng, Y. P. Greatly Enhanced Adsorption and Catalytic Activity of Au and Pt Clusters on Defective Graphene. *J. Chem. Phys.* **2010**, *132* (19), 194704.

(23) Yoo, E.; Okata, T.; Akita, T.; Kohyama, M.; Nakamura, J.; Honma, I. Enhanced Electrocatalytic Activity of Pt Subnanoclusters on Graphene Nanosheet Surface. *Nano Lett.* **2009**, *9* (6), 2255−2259.

(24) Yoo, E.; Okada, T.; Akita, T.; Kohyama, M.; Honma, I.; Nakamura, J. Sub-Nano-Pt Cluster Supported on Graphene Nanosheets for CO Tolerant Catalysts in Polymer Electrolyte Fuel Cells. *J. Power Sources* **2011**, *196* (1), 110−115.

DOI: 10.1021/acs.jpcc.8b06621
J. Phys. Chem. C 2018, 122, 21919−21926

(25) Kou, R.; Shao, Y.; Mei, D.; Nie, Z.; Wang, D.; Wang, C.; Viswanathan, V. V.; Park, S.; Aksay, I. A.; Lin, Y.; et al. Stabilization of Electrocatalytic Metal Nanoparticles at Metal−Metal Oxide−Graphene Triple Junction Points. *J. Am. Chem. Soc.* **2011**, *133* (8), 2541−2547.
(26) Guo, D.; Shibuya, R.; Akiba, C.; Saji, S.; Kondo, T.; Nakamura, J. Active Sites of Nitrogen-Doped Carbon Materials for Oxygen Reduction Reaction Clarified Using Model Catalysts. *Science* **2016**, *351* (6271), 361−365.
(27) Lai, L.; Potts, J.; Zhan, D.; Wang, L.; Kok Poh, C.; Tang, C.; Gong, H.; Shen, Z.; Lin, J.; Ruoff, R. S. Exploration of the Active Center Structure of Nitrogen-Doped Graphene-Based Catalysts for Oxygen Reduction Reaction. *Energy Environ. Sci.* **2012**, *5* (7), 7936−7942.
(28) Song, E. H.; Wen, Z.; Jiang, Q. CO Catalytic Oxidation on Copper-Embedded Graphene. *J. Phys. Chem. C* **2011**, *115* (9), 3678−3683.
(29) Li, Y.; Zhou, Z.; Yu, G.; Chen, W.; Chen, Z. CO Catalytic Oxidation on Iron-Embedded Graphene: Computational Quest for Low-Cost Nanocatalysts. *J. Phys. Chem. C* **2010**, *114* (14), 6250−6254.
(30) Lu, Y.-H.; Zhou, M.; Zhang, C.; Feng, Y.-P. Metal-Embedded Graphene: A Possible Catalyst with High Activity. *J. Phys. Chem. C* **2009**, *113* (47), 20156−20160.
(31) Okazaki-Maeda, K.; Morikawa, Y.; Tanaka, S.; Kohyama, M. Structures of Pt Clusters on Graphene by First-Principles Calculations. *Surf. Sci.* **2010**, *604* (2), 144−154.
(32) Blonski, P.; Hafner, J. Geometric and Magnetic Properties of Pt Clusters Supported on Graphene: Relativistic Density-Functional Calculations. *J. Chem. Phys.* **2011**, *134*, 154705.
(33) Fampiou, I.; Ramasubramaniam, A. Binding of Pt Nanoclusters to Point Defects in Graphene: Adsorption, Morphology, and Electronic Structure. *J. Phys. Chem. C* **2012**, *116* (11), 6543−6555.
(34) Alavi, A.; Hu, P.; Deutsch, T.; Silvestrelli, P. L.; Hutter, J. CO Oxidation on Pt(111): An Ab Initio Density Functional Theory Study. *Phys. Rev. Lett.* **1998**, *80* (16), 3650−3653.
(35) Eichler, A.; Hafner, J. Reaction Channels for the Catalytic Oxidation of CO on Pt(111). *Surf. Sci.* **1999**, *433*−*435*, 58−62.
(36) Bleakley, K.; Hu, P. A Density Functional Theory Study of the Interaction between CO and O on a Pt Surface: CO/Pt(111), O/Pt(111), and CO/O/Pt(111). *J. Am. Chem. Soc.* **1999**, *121* (33), 7644−7652.
(37) Chen, M. S.; Cai, Y.; Yan, Z.; Gath, K. K.; Axnanda, S.; Goodman, D. W. Highly Active Surfaces for CO Oxidation on Rh, Pd, and Pt. *Surf. Sci.* **2007**, *601* (23), 5326−5331.
(38) Šljivančanin, Ž.; Hammer, B. CO Oxidation on Fully Oxygen Covered Ru(0001): Role of Step Edges. *Phys. Rev. B: Condens. Matter Mater. Phys.* **2010**, *81* (12), 121413.
(39) Montemore, M. M.; van Spronsen, M. A.; Madix, R. J.; Friend, C. M. O2 Activation by Metal Surfaces: Implications for Bonding and Reactivity on Heterogeneous Catalysts. *Chem. Rev.* **2018**, *118* (5), 2816−2862.
(40) Wiebenga, M. H.; Kim, C. H.; Schmieg, S. J.; Oh, S. H.; Brown, D. B.; Kim, D. H.; Lee, J.-H.; Peden, C. H. F. Deactivation Mechanisms of Pt/Pd-Based Diesel Oxidation Catalysts. *Catal. Today* **2012**, *184* (1), 197−204.
(41) Kašpar, J.; Fornasiero, P.; Hickey, N. Automotive Catalytic Converters: Current Status and Some Perspectives. *Catal. Today* **2003**, *77* (4), 419−449.
(42) Chatterjee, D.; Deutschmann, O.; Warnatz, J. Detailed Surface Reaction Mechanism in a Three-Way Catalyst. *Faraday Discuss.* **2002**, *119* (0), 371−384.
(43) Bartholomew, C. H.; Farrauto, R. J. *Fundamentals of Industrial Catalytic Processes*, 2nd ed.; John Wiley & Sons, Inc., 2006.
(44) Liu, J.; Lucci, F. R.; Yang, M.; Lee, S.; Marcinkowski, M. D.; Therrien, A. J.; Williams, C. T.; Sykes, E. C. H.; Flytzani-Stephanopoulos, M. Tackling CO Poisoning with Single-Atom Alloy Catalysts. *J. Am. Chem. Soc.* **2016**, *138* (20), 6396−6399.
(45) Kresse, G.; Furthmüller, J. Efficiency of Ab-Initio Total Energy Calculations for Metals and Semiconductors Using a Plane-Wave Basis Set. *Comput. Mater. Sci.* **1996**, *6* (1), 15−50.
(46) Kresse, G.; Furthmüller, J. Efficient Iterative Schemes for Ab Initio Total-Energy Calculations Using a Plane-Wave Basis Set. *Phys. Rev. B: Condens. Matter Mater. Phys.* **1996**, *54* (16), 11169.
(47) Kresse, G.; Joubert, D. From Ultrasoft Pseudopotentials to the Projector Augmented-Wave Method. *Phys. Rev. B: Condens. Matter Mater. Phys.* **1999**, *59* (3), 1758.
(48) Blöchl, P. E. Projector Augmented-Wave Method. *Phys. Rev. B: Condens. Matter Mater. Phys.* **1994**, *50* (24), 17953−17979.
(49) Perdew, J. P.; Burke, K.; Ernzerhof, M. Generalized Gradient Approximation Made Simple. *Phys. Rev. Lett.* **1996**, *77* (18), 3865−3868.
(50) Monkhorst, H. J.; Pack, J. D. Special Points for Brillouin-Zone Integrations. *Phys. Rev. B* **1976**, *13* (12), 5188−5192.
(51) Momma, K.; Izumi, F. VESTA 3 for Three-Dimensional Visualization of Crystal, Volumetric and Morphology Data. *J. Appl. Crystallogr.* **2011**, *44* (6), 1272−1276.
(52) Henkelman, G.; Uberuaga, B. P.; Jónsson, H. A Climbing Image Nudged Elastic Band Method for Finding Saddle Points and Minimum Energy Paths. *J. Chem. Phys.* **2000**, *113* (22), 9901−9904.
(53) Henkelman, G.; Jónsson, H. Improved Tangent Estimate in the Nudged Elastic Band Method for Finding Minimum Energy Paths and Saddle Points. *J. Chem. Phys.* **2000**, *113* (22), 9978−9985.
(54) Sheppard, D.; Terrell, R.; Henkelman, G. Optimization Methods for Finding Minimum Energy Paths. *J. Chem. Phys.* **2008**, *128* (13), 134106.
(55) Sheppard, D.; Henkelman, G. Paths to Which the Nudged Elastic Band Converges. *J. Comput. Chem.* **2011**, *32* (8), 1769−1771.
(56) Sheppard, D.; Xiao, P.; Chemelewski, W.; Johnson, D. D.; Henkelman, G. A Generalized Solid-State Nudged Elastic Band Method. *J. Chem. Phys.* **2012**, *136* (7), 074103.
(57) Tison, Y.; Lagoute, J.; Repain, V.; Chacon, C.; Girard, Y.; Rousset, S.; Joucken, F.; Sharma, D.; Henrard, L.; Amara, H.; et al. Electronic Interaction between Nitrogen Atoms in Doped Graphene. *ACS Nano* **2015**, *9* (1), 670−678.
(58) Joucken, F.; Tison, Y.; Lagoute, J.; Dumont, J.; Cabosart, D.; Zheng, B.; Repain, V.; Chacon, C.; Girard, Y.; Botello-Méndez, A. R.; et al. Localized State and Charge Transfer in Nitrogen-Doped Graphene. *Phys. Rev. B: Condens. Matter Mater. Phys.* **2012**, *85* (16), 161408.
(59) Zhao, L.; He, R.; Rim, K. T.; Schiros, T.; Kim, K. S.; Zhou, H.; Gutiérrez, C.; Chockalingam, S. P.; Arguello, C. J.; Pálová, L.; et al. Visualizing Individual Nitrogen Dopants in Monolayer Graphene. *Science* **2011**, *333* (6045), 999−1003.
(60) Üzengi Aktürk, O.; Tomak, M. Au_nPt_n clusters adsorbed on graphene studied by first-principles calculations. *Phys. Rev. B: Condens. Matter Mater. Phys.* **2009**, *80* (8), 085417.
(61) Chi, D. H.; Cuong, N. T.; Tuan, N. A.; Kim, Y.-T.; Bao, H. T.; Mitani, T.; Ozaki, T.; Nagao, H. Electronic Structures of Pt Clusters Adsorbed on (5,5) Single Wall Carbon Nanotube. *Chem. Phys. Lett.* **2006**, *432* (1), 213−217.
(62) Ganji, M. D.; Sharifi, N.; Ardjmand, M.; Ahangari, M. G. Pt-Decorated Graphene as Superior Media for H2S Adsorption: A First-Principles Study. *Appl. Surf. Sci.* **2012**, *261*, 697−704.
(63) Krasheninnikov, A. V.; Lehtinen, P. O.; Foster, A. S.; Pyykkö, P.; Nieminen, R. M. Embedding Transition-Metal Atoms in Graphene: Structure, Bonding, and Magnetism. *Phys. Rev. Lett.* **2009**, *102* (12), 126807.
(64) Tang, Y.; Yang, Z.; Dai, X. Trapping of Metal Atoms in the Defects on Graphene. *J. Chem. Phys.* **2011**, *135* (22), 224704.
(65) Tang, Y.; Liu, Z.; Chen, W.; Shen, Z.; Li, C.; Dai, X. Theoretical Study on the Removal of Adsorbed Sulfur on Pt Anchored Graphene Surfaces. *Int. J. Hydrogen Energy* **2015**, *40* (21), 6942−6949.
(66) Błoński, P.; Hafner, J. Magnetic Anisotropy of Heteronuclear Dimers in the Gas Phase and Supported on Graphene: Relativistic

DOI: 10.1021/acs.jpcc.8b06621
J. Phys. Chem. C 2018, 122, 21919−21926

Density-Functional Calculations. *J. Phys.: Condens. Matter* **2014**, *26* (14), 146002.
(67) Wei, D.; Liu, Y.; Wang, Y.; Zhang, H.; Huang, L.; Yu, G. Synthesis of N-Doped Graphene by Chemical Vapor Deposition and Its Electrical Properties. *Nano Lett.* **2009**, *9* (5), 1752−1758.
(68) Schiros, T.; Nordlund, D.; Pálová, L.; Prezzi, D.; Zhao, L.; Kim, K. S.; Wurstbauer, U.; Gutiérrez, C.; Delongchamp, D.; Jaye, C.; et al. Connecting Dopant Bond Type with Electronic Structure in N-Doped Graphene. *Nano Lett.* **2012**, *12* (8), 4025−4031.
(69) Hammer, B.; Nielsen, O. H.; Nrskov, J. K. Structure Sensitivity in Adsorption: CO Interaction with Stepped and Reconstructed Pt Surfaces. *Catal. Lett.* **1997**, *46* (1−2), 31−35.
(70) Mostafa, S.; Behafarid, F.; Croy, J. R.; Ono, L. K.; Li, L.; Yang, J. C.; Frenkel, A. I.; Cuenya, B. R. Shape-Dependent Catalytic Properties of Pt Nanoparticles. *J. Am. Chem. Soc.* **2010**, *132* (44), 15714−15719.
(71) Kale, M. J.; Christopher, P. Utilizing Quantitative in Situ FTIR Spectroscopy To Identify Well-Coordinated Pt Atoms as the Active Site for CO Oxidation on Al2O3-Supported Pt Catalysts. *ACS Catal.* **2016**, *6* (8), 5599−5609.
(72) Tang, Y.; Yang, Z.; Dai, X.; Ma, D.; Fu, Z. Formation, Stabilities, and Electronic and Catalytic Performance of Platinum Catalyst Supported on Non-Metal-Doped Graphene. *J. Phys. Chem. C* **2013**, *117* (10), 5258−5268.
(73) Sun, S.; Zhang, G.; Gauquelin, N.; Chen, N.; Zhou, J.; Yang, S.; Chen, W.; Meng, X.; Geng, D.; Banis, M. N.; et al. Single-Atom Catalysis Using Pt/Graphene Achieved through Atomic Layer Deposition. *Sci. Rep.* **2013**, DOI: 10.1038/srep01775.
(74) Tang, Y.; Yang, Z.; Dai, X. A Theoretical Simulation on the Catalytic Oxidation of CO on Pt/Graphene. *Phys. Chem. Chem. Phys.* **2012**, *14* (48), 16566−16572.
(75) Holme, T.; Zhou, Y.; Pasquarelli, R.; O'Hayre, R. First Principles Study of Doped Carbon Supports for Enhanced Platinum Catalysts. *Phys. Chem. Chem. Phys.* **2010**, *12* (32), 9461−9468.
(76) Cheng, N.; Stambula, S.; Wang, D.; Banis, M. N.; Liu, J.; Riese, A.; Xiao, B.; Li, R.; Sham, T.-K.; Liu, L.-M.; et al. Platinum Single-Atom and Cluster Catalysis of the Hydrogen Evolution Reaction. *Nat. Commun.* **2016**, DOI: 10.1038/ncomms13638.
(77) Luo, Z.; Lim, S.; Tian, Z.; Shang, J.; Lai, L.; MacDonald, B.; Fu, C.; Shen, Z.; Yu, T.; Lin, J. Pyridinic N Doped Graphene: Synthesis, Electronic Structure, and Electrocatalytic Property. *J. Mater. Chem.* **2011**, *21* (22), 8038−8044.
(78) Groves, M. N.; Chan, A. S. W.; Malardier-Jugroot, C.; Jugroot, M. Improving Platinum Catalyst Binding Energy to Graphene through Nitrogen Doping. *Chem. Phys. Lett.* **2009**, *481* (4−6), 214−219.
(79) Zou, X.; Zhang, Y. Noble Metal-Free Hydrogen Evolution Catalysts for Water Splitting. *Chem. Soc. Rev.* **2015**, *44* (15), 5148−5180.
(80) Cheng, N.; Stambula, S.; Wang, D.; Banis, M. N.; Liu, J.; Riese, A.; Xiao, B.; Li, R.; Sham, T.-K.; Liu, L.-M.; et al. Platinum Single-Atom and Cluster Catalysis of the Hydrogen Evolution Reaction. *Nat. Commun.* **2016**, DOI: 10.1038/ncomms13638.
(81) Brix, P.; Herzberg, G. The Dissociation Energy of Oxygen. *J. Chem. Phys.* **1953**, *21* (12), 2240−2240.

DOI: 10.1021/acs.jpcc.8b06621
J. Phys. Chem. C 2018, 122, 21919−21926